

Spatially heterogenous dynamics in dense, driven granular flows

Allison Ferguson, Bulbul Chakraborty

Martin Fisher School of Physics, Brandeis University, Mailstop 057, Waltham, MA 02454-9110, USA

(Dated: August 14, 2018)

Interest in the dynamical arrest leading to a fluid \rightarrow solid transition in thermal and athermal systems has led to questions about the nature of these transitions. These jamming transitions may be dependent on the influence of extended structures on the dynamics of the system. Here we show results from a simple driven, dissipative, non-equilibrium system which exhibits dynamical heterogeneities similar to those observed in a supercooled liquid which is a system in thermal equilibrium. Observations of the time $\tau_R(r)$ required for a particular particle to move a distance r reveal the existence of large-scale correlated dynamical regions with characteristic timescales chosen from a broad distribution. The mean squared displacement of ensembles of particles with varying characteristic $\tau_R(r)$ reveals an intriguing spatially heterogenous mobility. This suggests that a unified framework for jamming will have to be based on the connection between the nature of these heterogeneities and the effective dynamics.

PACS numbers: 81.05.Rm, 45.70.-n, 83.10.Pp

I. INTRODUCTION

Materials as diverse as molecular liquids, foams and granular matter experience a transition from a fluid-like state to a solid-like state characterized only by a sudden arrest of their dynamics. It has been proposed that the phenomena associated with this dynamical arrest can be explained within the unified framework of a jamming phase diagram [1]. Unlike thermal phase transitions, jamming does not seem to be characterized by singularities in any purely static, structural property [2, 3]. Numerous experiments and simulations indicate the appearance of large-scale dynamical heterogeneities and an associated growing dynamical length scale. In colloids near the glass transition, for example, fast-moving particles were observed to be spatially correlated with a characteristic cluster size that increased as the glass transition was approached [4]. In supercooled liquids, spatial inhomogeneities can be identified via a time-dependent four-point (two-time, two-space) correlation function [5]. Recent experiments on molecular liquids and colloids have identified a growing dynamical length scale near the glass transition via new multipoint dynamic susceptibilities [6]. In granular materials, spatial structures have been directly observed in experiments on flowing systems [7, 8]. More recently, measurements of velocity correlations in the surface layer of particles flowing down an inclined plane have yielded a length scale which appears to grow as the flow is arrested [9]. While detection of such dynamical heterogeneities in numerical studies has been more difficult, extended chains of particles experiencing high frequency collisions are visible in event-driven simulations of gravity driven granular flow [10]. These structures experience a slow relaxation from collisional stress at intermediate time scales in a manner analogous to temporal relaxations observed in glassy systems at low temperatures [11]. There is also some evidence for the existence of large-scale structure in images of the contact force network in simulations of chute flow [12].

Several questions naturally arise: (1) Are dynamical heterogeneities a necessary precursor to dynamical arrest of the jamming kind? (2) Do these heterogeneities and their mesoscopic scale lead to any kind of universal dynamical behavior irrespective of significant differences in microscopic dynamics? (3) Do static structures such as force chains observed in jammed granular packings emerge out of dynamical heterogeneities?

In the present work we address these questions via a simplified model which focuses on the essential effects of driving and dissipation in a flowing granular system. Simulations have been performed of a two-dimensional gravity driven system of frictionless bidisperse hard disks in a hopper geometry. The disks undergo instantaneous, inelastic binary collisions and propagate under gravity in between collisions; a driven, dissipative system that is very different from supercooled molecular liquids. Previous work [10] has shown that this minimal model still reproduces observable results from related experimental systems [13]. To investigate the relevant time and length scales governing the dynamics of the granular system, an interesting analysis for quantifying dynamical heterogeneity in non-equilibrium systems [14] independent of the microscopic interactions between particles is employed. Specifically, measurements of the time $\tau_R(r)$ required for a particular particle to move a specified distance r , provide an appealing physical picture of large-scale correlated regions with characteristic timescales chosen from a broad distribution. Through a coarsegraining scheme first proposed in Ref. [14] which exploits the fact that the visible heterogeneity is maximized at a particular distance r_c , both the distance r_c (which can be associated with average cage size) and the spatial extent of the correlated regions ξ^* are extracted in a completely threshold-independent way. r_c can then be used to explore the effect of complex collective behaviour on dynamic properties such as the average mean squared displacement $\langle(\Delta r)^2\rangle$.

II. METHODS

The grain dynamics used in the simulations are similar to Ref. [15]. Specifically, (i) at each interparticle collision, momentum is conserved but the collisions are inelastic so the relative normal velocity is reduced by the coefficient of restitution μ ; (ii) to allow the side walls to absorb some vertical momentum we impose the condition that collisions with the walls are inelastic with a coefficient of restitution μ_{wall} in the direction tangential to the wall and (iii) since we wish to observe the system over many events, particles exiting the system at the bottom must be replaced at the top to create uniform, sustained flow. Note that collisions are instantaneous and in between collisions the particles are driven by gravity. To avoid the phenomena of inelastic collapse the coefficients of restitution μ and μ_{wall} are velocity dependent; if the relative normal velocity between particles or between a given particle and the wall is less than some cutoff v_{cut} then the collision is presumed to be elastic [16]. The flow velocity v_f is controlled by adjusting the width of the hopper opening. We also introduce a probability of reflection p at the bottom which reduces the time needed to reach steady-state flow. Typically, our simulations were done on bidisperse systems (diameter ratio 1:1.2) of 1000 disks, with $\mu = 0.8$, $\mu_{wall} = 0.5$, $v_{cut} = 1 \times 10^{-3}$ and $p = 0.5$. The simulation was run for a total time of 1×10^3 in simulation time units (smaller particle diameter d_s , smaller particle mass m_s and gravitational constant g are all set to 1) with the initial time interval of 5×10^2 discarded before recording data to ensure the system has reached steady state. During the total time interval of 500 over which we are evaluating the data, a given particle will pass through the hopper 5-10 times depending on the flow velocity.

III. RELAXATION TIMES AND CAGE-BREAKING FLUCTUATIONS

Subdiffusive behavior and caging have become hallmarks of the jamming transition, but defining a quantitative measure for these processes which is sensitive to the presence of dynamical heterogeneity has been difficult. The following observation suggests a possible procedure for defining a characteristic time for a particular particle which may detect the presence of any spatial heterogeneity in the dynamics: if the relaxation time $\tau_R^i(r)$ of a given particle i is defined as the time required for particle i to travel a distance r , then any spatial correlation in $\tau_R^i(r)$ (given initial positions of the particles) will depend very strongly on the chosen value of r . If r is small, then it is not possible to distinguish between those particles which are simply rattling back and forth within some confined distance and those which may have some enhanced motility. On the other hand, if r is too large, then a given particle i may have been in regions where the local average relaxation time has taken on many val-

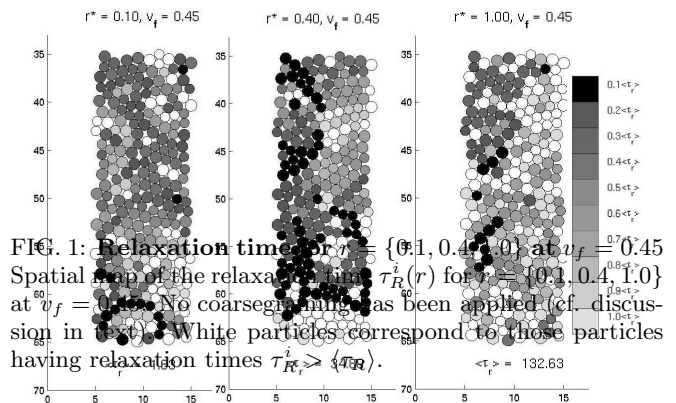


FIG. 1: Relaxation times for $r = \{0.1, 0.4, 1.0\}$ at $v_f = 0.45$. Spatial map of the relaxation times $\tau_R^i(r)$ for $r = \{0.1, 0.4, 1.0\}$ at $v_f = 0.45$. No coarsegraining has been applied (cf. discussion in text). White particles correspond to those particles having relaxation times $\tau_R^i > \langle \tau_R \rangle$.

ues, both fast and slow. In both cases, a spatial map of the relaxation time reveals no clear positional correlation in regions of $\tau_R^i(r)$ beyond some small length scale associated with random clumping (Fig. 1a and c, respectively).

However, at some intermediate value of r , it should be possible to distinguish between localized motion and extended translational motion prior to a “washing-out” of any spatial correlations between particles with similar relaxation times (compare Fig. 1b, where $r = 0.45$ to Fig. 1a and c, and note the clearer distinction between regions with different $\tau_R^i(r)$). Presumably there is some optimal value r_c at which the visible heterogeneity in $\tau_R(r)$ is maximized. The primary aim of the analysis proposed in Ref. [14] is to determine this value of r_c and thence the distribution of “critical” relaxation times $P(\tau_R^c)$ where $\tau_R^c = \tau_R(r_c)$. Particle behaviour such as mean squared displacement can then be analyzed in the context of τ_R^c for each individual grain and whether or not the particle is then “fast” or “slow”.

The method for determining the critical relaxation length r_c is as follows: Define the coarsegrained relaxation time $\tau_R^i(r, l)$ for a given particle i as the mean local relaxation time in a box of size $l \times l$ centered on particle i . As the size of the coarse-graining region is varied from $l = 1$ (essentially, the single particle relaxation time) to the size of the analysis region $l = L$, the spatial variation in $\tau_R^i(r, l)$ should decrease (the result of the coarsegraining procedure on the spatial map is depicted for one snapshot of the system in Fig. 2 for coarsegraining lengths of $l = 2, 5, 10$). Thus, the distribution $P(\tau_R(r, l))$ should become increasingly narrower, having zero width at $l = L$ where all of the $\tau_R^i(r, L) = \frac{1}{N} \sum_i \tau_R^i(r, 1) = \overline{\tau_R}$. It is clear from the picture that the heterogeneities persist up to larger l for $r \sim 0.4$. If the second cumulant $m_2(r, l)$ of

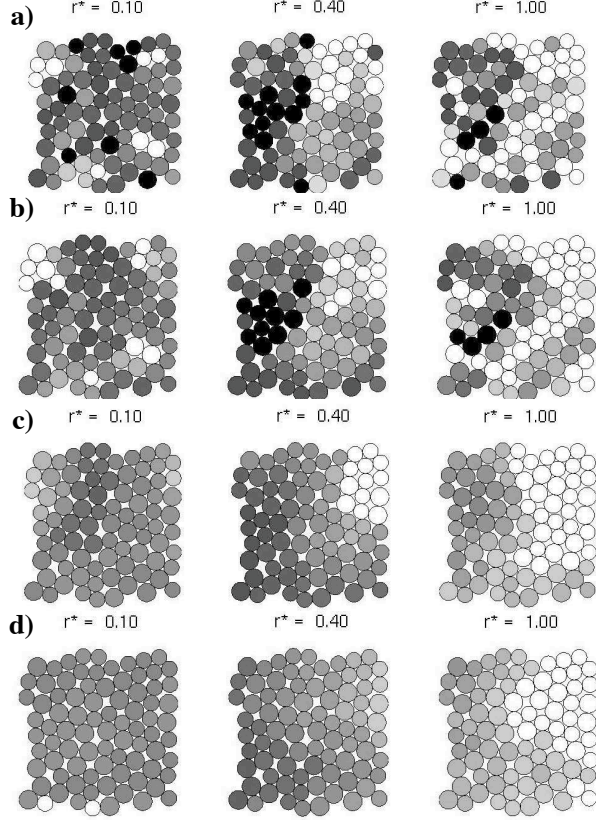


FIG. 2: **Effect of coarsegraining on relaxation time map** for $r = \{0.1, 0.4, 1.0\}$. Spatial map of the relaxation time $\tau_r(r, l)$ for $r = \{0.1, 0.4, 1.0\}$ at $v_f = 0.45$ for (a) no coarsegraining ($l = 1$), (b) $l = 2$, (c) $l = 5$ and (d) $l = 10$. Colour scale is as for Fig. 1.

$P(\tau_R(r, l))$ is calculated as:

$$m_2(r, l) = \frac{\langle (\tau_R^i(r, l) - \overline{\tau_R})^2 \rangle}{\langle (\tau_R^i(r, 1) - \overline{\tau_R})^2 \rangle} \quad (1)$$

then $m_2(r, l)$ should be a monotonically decreasing function of l , where the length scale associated with the decay of $m_2(r, l)$ should vary with r and be maximal at r_c .

It is worth noting at this point that the original measurement performed in Ref. [14] was for a 2D periodic system of soft particles in thermal equilibrium interacting via the repulsive potential $V(r) = \epsilon(\sigma/r)^{-12}$. While the validity of this analysis should not depend on the type of microscopic interaction between particles, two additional considerations had to be taken into account before performing this calculation on the flowing granular system. Firstly, motion due to the net flow of the system had to be subtracted off prior to calculating $\tau_R^i(r, l)$. While more complicated schemes involving a spatially varying flow field could be devised to more accurately compensate for this effect, for the analysis here the velocity over the region of interest $v_f(t)$ was assumed to be constant in space at the snapshot at time t (*i.e.* so a particle's

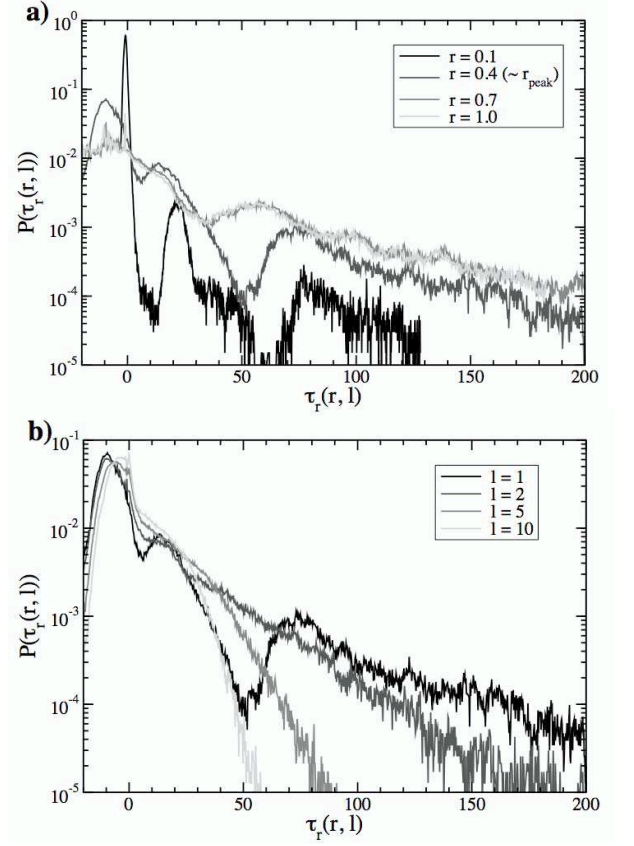


FIG. 3: **Relaxation time distributions** $P(\tau_R(r, l))$ for $v_f = 1.13$. Relaxation time distributions $P(\tau_R(r, l))$ for (a) $r = 0.4$ ($\sim r_c$ for this flow velocity) and (b) $l = 1$ for $r = \{0.1, 0.4, 0.7, 1.0\}$. In all cases the distributions are for $v_f = 1.13$ and the average relaxation time $\overline{\tau_R}$ has been subtracted off. Note that the average collision time for this flow velocity is $\tau \sim 1 \times 10^{-3}$ and thus typical relaxation times are $\gg \tau$.

displacement $\Delta \mathbf{r}(t)$ in a given time interval Δt is calculated as $\Delta \mathbf{r}(t) = \mathbf{r}(t) - \mathbf{r}(t - \Delta t) - v_f(t - \Delta t)\Delta t$). This first approximation seemed to be sufficient to extract r_c . Secondly, because relaxation times were only calculated for particles in the constant flow region, not all particles in the system will be in this region at a given time, nor will a given particle necessarily remain in the region of interest until it reaches the specified value of r . So the calculation only considers a given particle trajectory until it departs the analysis region.

Relaxation time distributions $P(\tau_R(r, l))$ for $r = 0.4$ and $l = \{1, 2, 5, 10\}$ are shown in Fig. 3a, with a comparison of the single-particle (*i.e.*, $l = 1$) relaxation time for several values of r in Fig. 3b. The effect of increasing the coarsegraining region for a given value of r is to smooth out the distribution for $\tau_R(r, l) > \overline{\tau_R}$, and the width of the distribution decreases as expected for increasing l . Note that the single particle distribution for $l = 1$ can be quite broad for large values of r . This is a reasonable re-

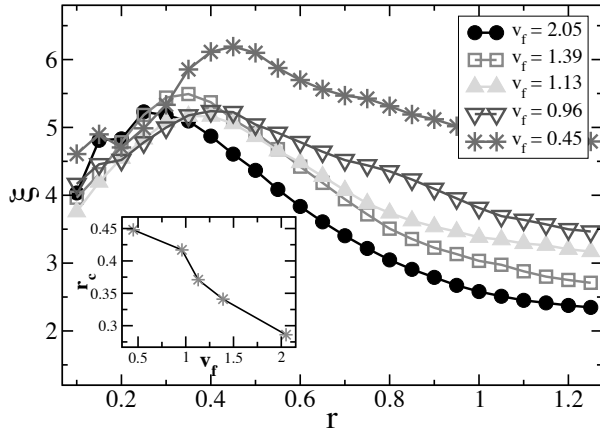


FIG. 4: $\xi(r)$ for varying v_f . Decay length scale $\xi(r) = \int_1^L m_2(l, r) dl$ as a function of r for varying v_f . Inset shows peak location r_c vs. v_f .

sult in the context of the calculation of r_c ; the individual distributions for a particular value of $r \neq r_c$ can be broad initially, but unless there is any significant spatial correlation in relaxation times the spatial structure of $\tau_R(r, l)$ will vanish rapidly with increasing l compared to a value of r with nontrivial spatial correlations. Thus the utility of $\tau_R(r, l)$ lies in its ability to emphasize spatial correlations between fast and slow particles (*i.e.* if there are particles of widely different mobilities in the system but they were randomly distributed in space then no interesting correlation length is visible).

The length scale associated with the decay of $m_2(l, r)$ can be calculated from $\xi(r) = \int_1^L m_2(l, r) dl$. As can be clearly seen in Fig. 4, there is a distinct peak in $\xi(r)$ from which two separate and interesting length scales can be extracted. One is the location in r of the peak; this quantity is r_c and it is the length scale over which the dynamical heterogeneity in relaxation times is maximized as described above. An additional interpretation can be made of r_c as the critical fluctuation associated with cage-breaking in supercooled fluids (or equivalently, the typical cage size). This was proposed in Ref. [14] and confirmed experimentally for slow, quasistatic granular shear flows in Ref. [17]. Referring to the inset to Fig. 4, this quantity is decreasing monotonically with flow velocity, although the exact functional form is difficult to determine. It is also important to note that because r_c can be related back to a critical relaxation time, changes in r_c with v_f will correspond to changes in the distribution of τ_R^c .

The second length scale which may be determined from $\xi(r)$ is the peak height ξ^* , which represents the average size of the heterogeneity. From Fig. 4, it is difficult to determine if ξ^* is varying with v_f , or varying very slowly compared to the changes in r_c . This is in contrast to the results of Ref. [14] where an increase in density pro-

duced an increase in ξ^* while r_c remained fixed. Thus the crucial length scale which is growing as the flow velocity decreases in our system appears to be r_c . There is some indication of a crossover between a low-velocity regime where ξ may be changing more rapidly than r_c to a high-velocity regime where changes in r_c dominate as described above, but the current data is not sufficient to quantitatively distinguish between these two possibilities. Additionally, the effect of the finite size of the system on the dynamically correlated regions remains an interesting unresolved issue. While the correlation lengths measured over the range of flow velocities measured here are still sufficiently smaller than the system dimension, certainly at the slowest flow velocity observed the size of these regions begins to approach the system size (at least in the direction perpendicular to the flow). In order to fully observe the behaviour of this length scale as the flow velocity is decreased further, it will be necessary to use larger systems.

IV. SPATIALLY HETEROGENOUS MOBILITY

With the critical fluctuation r_c determined, the critical relaxation time τ_R^c for each particle can be defined (Fig. 1b shows a snapshot of the $v_f = 0.45$ system at $r = r_c$). As in Ref. [14], different particles can now be grouped into subsets according to their value of τ_R^c and the contribution of these subsets to dynamical measures (in this case, the mean squared displacement (MSD) $\langle \Delta r^2 \rangle$) can be evaluated. Plots of $\langle \Delta r^2 \rangle$ vs. time are shown in Fig. 5 for varying flow rates (the distributions of critical relaxation times for a given flow rate are shown in the insets to Fig. 5). In all cases, the MSD averaged over all particles in the system in the short-time regime is approximately ballistic ($\langle \Delta r^2 \rangle \sim t^{1.8}$). The long time power-law behaviour is characterized by a flow velocity dependent exponent ($\langle \Delta r^2 \rangle \sim t^{\gamma(v_f)}$, where $0.9 < \gamma(v_f) < 1.2$ in the range of flow velocities studied) which is nearly diffusive. Fig. 5a shows the power-law fits to the mean squared displacement curves for two different flow velocities. At times comparable to the average time it takes a particle to cross the analysis region $t_{\text{cross}} = l/v_f$, the particle falls out of the dense constant flow velocity region and accelerates under gravity, leading to the sharp increase in the mean squared displacement at $t \sim t_{\text{cross}}$.

The MSD curves for “slow” ($\tau_R^c \sim t_{\text{cross}}$) and “fast” ($\tau_R^c \sim (1/3 - 1/2) t_{\text{cross}}$) particles reveal a deeper complexity not visible in the mean squared displacement averaged over the system as a whole. As $v_f \rightarrow 0$, these two groups of particles show increasing separation from the average MSD, with the fast particles experiencing greater displacement than the average in a given time interval, and the slow particles exhibiting a plateau (Fig. 5b-c). For the slowest flow velocity measured, where the plateau is best defined, the plateau occurs at $\langle \Delta r^2 \rangle \sim r_c^2$, corresponding to the experimental result of Ref. [17] where

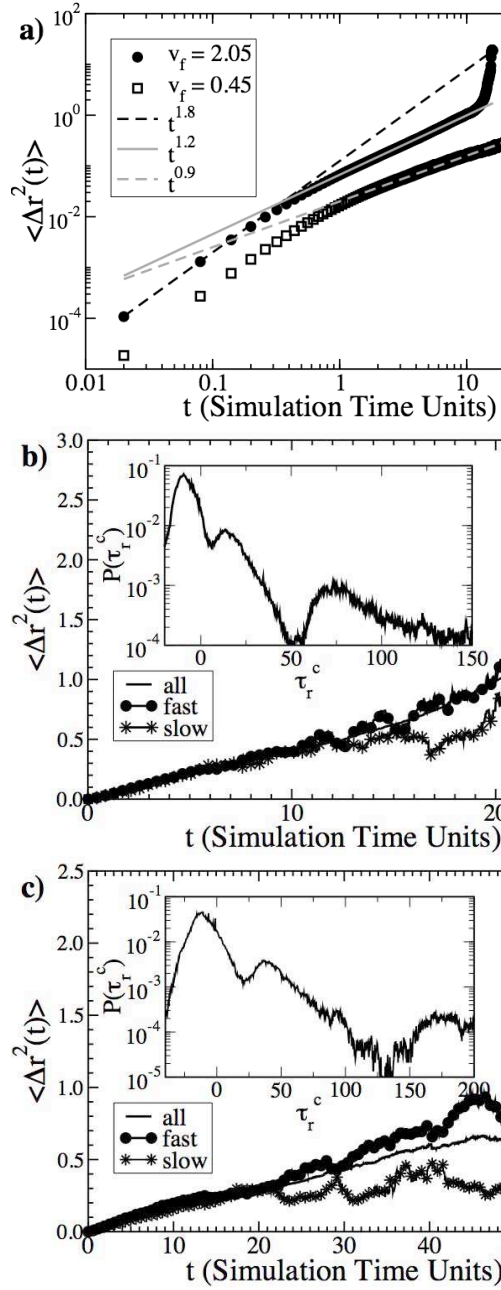


FIG. 5: Mean squared displacement $\langle \Delta r^2 \rangle$ for varying v_f . (a) Mean squared displacement (MSD) $\langle \Delta r^2 \rangle$ ($\langle \rangle$ indicates average over all particles in a snapshot at time t_0 , then average over all snapshots t_0) for $v_f = 2.05$ and $v_f = 0.45$. (b)-(c) Comparison of “slow” particles ($\tau_R^c \sim t_{cross}$) and “fast” particles ($\tau_R^c \sim 1/3 - 1.2 t_{cross}$) to the average over all particles (cf. discussion in text) for (b) $v_f = 1.13$ and (c) $v_f = 0.45$.

r_c has been directly associated with the cage size. Thus the overall transport in this system is governed by the dynamical heterogeneity: fast and slow regions are evident as depicted pictorially in Fig. 1 with particles in the slow region experiencing caging. As the flow velocity decreases, and the length scale r_c increases, the effect of these mesoscopic regions becomes more pronounced, with the slow particles at $v_f = 0.45$ remaining caged for the duration of their time to flow through the system (recall that for all of these displacement measurements motion due to the average flow has been subtracted off). This picture of rich collective dynamics occurring even in the absence of any evident density fluctuations was also suggested by Menon and Durian in experiments on dense gravity-driven granular flow using diffusing wave spectroscopy (DWS) [18]. This is also in analogy to the MSD for the Lennard-Jones system of Ref. [14], where slow particles (defined as the particles in the slowest 40% of $P(\tau_R)$) were seen to be caged over some time τ_{mix} during which the fast particles experienced diffusion with a diffusion constant twice that of the assembly of disks as a whole.

V. CONCLUSIONS

In summary, an interesting analysis for quantifying dynamical heterogeneity in non-equilibrium systems [14] independent of the microscopic interactions between particles has proven to be a useful tool for further investigation into the relevant time and length scales governing the dynamics of the gravity-driven granular system. Measurements of relaxation time $\tau_R(r)$, defined as the time required for a particular particle to move a specified distance r , provide an appealing physical picture of large-scale correlated regions with characteristic timescales chosen from a broad distribution of relaxation times $P(\tau_R)$. Through a clever coarsegraining scheme which exploits the fact that the visible heterogeneity is maximized at a particular distance r_c , both the distance r_c (which can be associated with average cage size) and the spatial extent of the correlated regions ξ^* were extracted in a completely threshold-independent way. While ξ^* was shown to be $\sim 5 - 6d$ independent of flow velocity, the cage size r_c grows as the flow velocity decreases. r_c then specifically defines the critical distribution of relaxation times $P(\tau_R^c)$ which can be used to explore the effect of complex collective behaviour on dynamic properties such as the average mean squared displacement $\langle (\Delta r)^2 \rangle$. The MSD in turn reveals a non-trivial spatial dependence in the mobility, indicating that while the total mean squared displacement at long times may seem approximately diffusive, there is underlying complexity in the form of “fast” and “slow” regions in the sample. This result is in agreement with several experimental studies on dense, driven granular materials [17, 18] and other jamming systems [4]. Additionally, there is a qualitative resemblance between the spa-

tial maps of relaxation time near the critical value τ_R^c (*c.f.* Fig. 1b) and recent measures of dynamic propensity and local Debye-Waller factors in 2D simulations of glass-formers [19].

One as yet unresolved puzzle is the relationship between the frequent-collision/high-stress chains identified in previous studies [10, 11] and the mesoscopic clumps of fast and slow particles characterized by a particular value of τ_R^c . From observations of the spatial map of collision frequency and critical relaxation time at a given snapshot of the system (not shown) it is difficult to ascertain if there is any correlation between the chains and regions of varying τ_R^c ; indeed, there can still be strong heterogeneity in the critical relaxation time in the absence of any chains. One measureable connection is that $\langle \tau_R^c \rangle \sim 1/v_f$, which is the same scaling with flow velocity that was measured

in the stress autocorrelations in Ref. [11] and associated with the lifetime of the chains. Thus $\tau_R v_f = \text{constant}$ could be an important clue to the dynamical principles leading to the heterogeneities, and may provide some additional insight into the reasons for why the frequently-colliding/high-stress chains form in these dense granular systems.

Acknowledgments

AF and BC acknowledge support from NSF through grants No. DMR 0207106 and DMR 0549762, and AF acknowledges support from the Natural Sciences and Engineering Research Council, Canada.

-
- [1] A. J. Liu and S. R. Nagel, *Nature* **396**, 21 (1998).
 - [2] H.M. Jaeger, S.R. Nagel and R.P. Behringer, *Rev. Mod. Phys.*, **68**, 1259 (1996).
 - [3] L.P. Kadanoff, *Rev. Mod. Phys.*, **71**, 435 (1999).
 - [4] E. Weeks *et al.*, *Science*, **287** 627 (2000).
 - [5] S. C. Glotzer, V. N. Novikov and T. B. Schroder, *J. Chem. Phys.* **112**, 509 (2000).
 - [6] L. Berthier, *et al.*, *Science* **310** 1797 (2005).
 - [7] D. Bonamy *et al.*, *Phys. Rev. Lett.* **89**, 034301 (2002).
 - [8] B. Miller, C. O'Hern and R. P. Behringer, *Phys. Rev. Lett.* **77** 3110 (1996).
 - [9] O. Pouliquen, *Phys. Rev. Lett.* **93**, 248001 (2004).
 - [10] A. Ferguson, B. Fisher and B. Chakraborty, *Europhys. Lett.* **66**, 277 (2004).
 - [11] A. Ferguson and B. Chakraborty, *Phys. Rev. E* **73** 011303 (2006).
 - [12] L. E. Silbert, *Phys. Rev. Lett.* **94** 098002 (2005).
 - [13] E. Longhi, N. Easwar and N. Menon, *Phys. Rev. Lett.* **89**, 045501 (2002).
 - [14] M. M. Hurley and P. Harrowell, *Phys. Rev. E* **52** 1694 (1995).
 - [15] C. Denniston and H. Li, *Phys. Rev. E* **59**, 3289 (1999).
 - [16] E. Ben-Naim, S.Y. Chen, G.D. Doolen, S. Redner, *Phys. Rev. Lett.* **83**, 4069 (1999).
 - [17] G. Marty and O. Dauchot, *Phys. Rev. Lett.* **94** 015701 (2005).
 - [18] N. Menon and D. J. Durian, *Science* **275** 1920 (1997).
 - [19] A. Widmer-Cooper and P. Harrowell, *Phys. Rev. Lett.* **96** 185701 (2006).